

Incorporating biological factors in radiation therapy treatment planning

Mark Brooke
DPhil Student

¹ *CRUK/MRC Oxford Institute for Radiation Oncology
University of Oxford*

Supervisors:

Prof. Frank van den Heuvel
Prof. Maria Hawkins
Dr. Francesca Fiorini

Presented at Loma Linda University
August 08 2018



Motivation

- ▶ PTCOG: as of end of 2014 over 137,000 cancer patients had been treated with particle therapy worldwide, with protons being the chosen modality in 86% of cases [Jermann, 2015]

Motivation

- ▶ PTCOG: as of end of 2014 over 137,000 cancer patients had been treated with particle therapy worldwide, with protons being the chosen modality in 86% of cases [Jermann, 2015]
- ▶ Main therapeutic advantage: *Bragg peak* in energy deposition

Motivation

- ▶ PTCOG: as of end of 2014 over 137,000 cancer patients had been treated with particle therapy worldwide, with protons being the chosen modality in 86% of cases [Jermann, 2015]
- ▶ Main therapeutic advantage: *Bragg peak* in energy deposition
- ▶ Most of the energy is deposited toward the end of its trajectory in a sharp peak

Motivation

- ▶ PTCOG: as of end of 2014 over 137,000 cancer patients had been treated with particle therapy worldwide, with protons being the chosen modality in 86% of cases [Jermann, 2015]
- ▶ Main therapeutic advantage: *Bragg peak* in energy deposition
- ▶ Most of the energy is deposited toward the end of its trajectory in a sharp peak
- ▶ Advantageous in IMPT as the energy and intensity of individual pencil beams can be manipulated to deposit a highly conformable dose to the tumour volume, with a low dose on entry and no exit dose

Motivation

- ▶ However the physical concept of dose – energy per unit mass – does not on its own adequately describe tumour control and normal tissue complications in particle therapy

Motivation

- ▶ However the physical concept of dose – energy per unit mass – does not on its own adequately describe tumour control and normal tissue complications in particle therapy
- ▶ Densely ionising particle tracks offer an increased cell-killing efficiency over sparsely ionising x-rays

Motivation

- ▶ However the physical concept of dose – energy per unit mass – does not on its own adequately describe tumour control and normal tissue complications in particle therapy
- ▶ Densely ionising particle tracks offer an increased cell-killing efficiency over sparsely ionising x-rays
- ▶ May be quantified through various biological endpoints

Motivation

- ▶ However the physical concept of dose – energy per unit mass – does not on its own adequately describe tumour control and normal tissue complications in particle therapy
- ▶ Densely ionising particle tracks offer an increased cell-killing efficiency over sparsely ionising x-rays
- ▶ May be quantified through various biological endpoints
- ▶ Quantification of radiobiological effects can be incorporated into treatment plan optimization algorithms

Motivation

- ▶ However the physical concept of dose – energy per unit mass – does not on its own adequately describe tumour control and normal tissue complications in particle therapy
- ▶ Densely ionising particle tracks offer an increased cell-killing efficiency over sparsely ionising x-rays
- ▶ May be quantified through various biological endpoints
- ▶ Quantification of radiobiological effects can be incorporated into treatment plan optimization algorithms
- ▶ Seek a dose distribution that is both physically and biologically favourable

Quantification of biological effects

Relative Biological Effectiveness

Definition

Relative Biological Effectiveness (RBE): the dose delivered using a specific modality and energy that yields the same biological effect as a reference dose in a reference modality;

$$\text{RBE}_{\langle \text{endpoint} \rangle} = \frac{\text{Dose of reference radiation}}{\text{Dose of test radiation}}. \quad (1)$$

Quantification of biological effects

Relative Biological Effectiveness

Definition

Relative Biological Effectiveness (RBE): the dose delivered using a specific modality and energy that yields the same biological effect as a reference dose in a reference modality;

$$\text{RBE}_{\langle \text{endpoint} \rangle} = \frac{\text{Dose of reference radiation}}{\text{Dose of test radiation}}. \quad (1)$$

- ▶ Commonly used endpoint is the number of surviving cells in a culture by clonogenic survival assay following irradiation

Quantification of biological effects

Relative Biological Effectiveness

Definition

Relative Biological Effectiveness (RBE): the dose delivered using a specific modality and energy that yields the same biological effect as a reference dose in a reference modality;

$$\text{RBE}_{\langle \text{endpoint} \rangle} = \frac{\text{Dose of reference radiation}}{\text{Dose of test radiation}}. \quad (1)$$

- ▶ Commonly used endpoint is the number of surviving cells in a culture by clonogenic survival assay following irradiation
- ▶ In-vivo prediction of the RBE, however, is required for radiation therapy

Quantification of biological effects

Relative Biological Effectiveness

Definition

Relative Biological Effectiveness (RBE): the dose delivered using a specific modality and energy that yields the same biological effect as a reference dose in a reference modality;

$$\text{RBE}_{\langle \text{endpoint} \rangle} = \frac{\text{Dose of reference radiation}}{\text{Dose of test radiation}}. \quad (1)$$

- ▶ Commonly used endpoint is the number of surviving cells in a culture by clonogenic survival assay following irradiation
- ▶ In-vivo prediction of the RBE, however, is required for radiation therapy
- ▶ In-vitro cell data on its own is unsatisfactory

Quantification of biological effects

Relative Biological Effectiveness

- ▶ Major mechanism for cell kill is believed to be the induction of double strand breaks (DSBs) in nuclear DNA [[Caldecott, 2008](#); [Ward, 1985](#)]

Quantification of biological effects

Relative Biological Effectiveness

- ▶ Major mechanism for cell kill is believed to be the induction of double strand breaks (DSBs) in nuclear DNA [[Caldecott, 2008](#); [Ward, 1985](#)]
- ▶ we choose to define a restricted RBE for complex damage based on DSB induction

Quantification of biological effects

Relative Biological Effectiveness

- ▶ Major mechanism for cell kill is believed to be the induction of double strand breaks (DSBs) in nuclear DNA [[Caldecott, 2008](#); [Ward, 1985](#)]
- ▶ we choose to define a restricted RBE for complex damage based on DSB induction

Quantification of biological effects

Relative Biological Effectiveness

- ▶ Major mechanism for cell kill is believed to be the induction of double strand breaks (DSBs) in nuclear DNA [Caldecott, 2008; Ward, 1985]
- ▶ we choose to define a restricted RBE for complex damage based on DSB induction

Definition

Restricted RBE for complex damage: ratio of the number of DSBs in the modality of interest to the number generated in a reference modality depositing the same dose;

$$\text{RBE}_{\text{cd}} = \left(\frac{\# \text{DSB induced by test radiation}}{\# \text{DSB induced by test radiation}}_{\text{same dose}} \right) \cdot \quad (2)$$

Modeling DNA damage

Linear energy transfer (LET)

- ▶ Differential loss of kinetic energy over distance given by stopping power $\langle dE/dl \rangle$

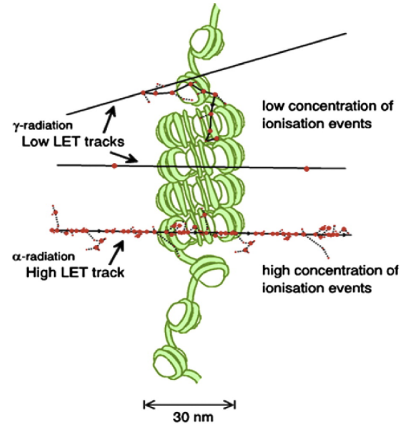


Figure: Image cropped from Fig 1 in [Lomax et al., 2013].

Modeling DNA damage

Linear energy transfer (LET)

- ▶ Differential loss of kinetic energy over distance given by stopping power $\langle dE/dl \rangle$
- ▶ Microdosimetry: linear energy transfer (LET) is used instead – which is stopping power but with energy delivered to highly energetic knock-on electrons subtracted

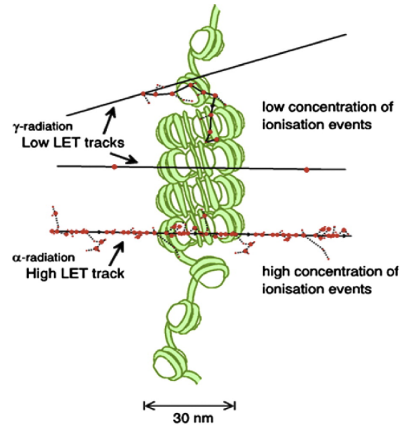


Figure: Image cropped from Fig 1 in [Lomax et al., 2013].

Modeling DNA damage

Linear energy transfer (LET)

- ▶ Differential loss of kinetic energy over distance given by stopping power $\langle dE/dl \rangle$
- ▶ Microdosimetry: linear energy transfer (LET) is used instead – which is stopping power but with energy delivered to highly energetic knock-on electrons subtracted
- ▶ Density of ionisations along track can therefore be measured using LET and is closely related to the kinetic energy of the particle

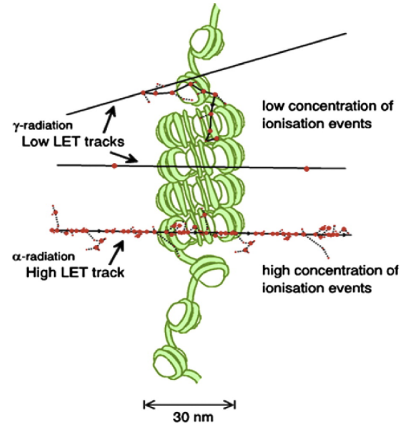


Figure: Image cropped from Fig 1 in [Lomax et al., 2013].

Modeling DNA damage

Single particle interaction model

- ▶ Approximate a section of the DNA as a cylinder

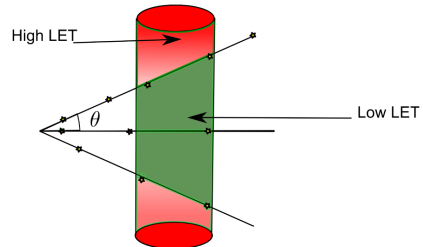


Figure: Image from Figure 1 in [Van den Heuvel, 2014].

Modeling DNA damage

Single particle interaction model

- ▶ Approximate a section of the DNA as a cylinder
- ▶ Use the energy dependent mean free path $\lambda(E)$ between successive ionisations to determine the distribution of clustered lesions [Van den Heuvel, 2014]

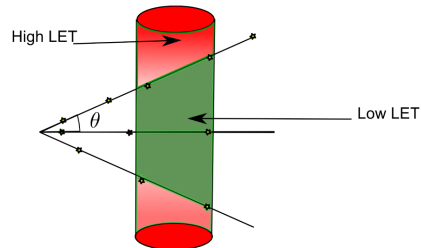


Figure: Image from Figure 1 in [Van den Heuvel, 2014].

Modeling DNA damage

Single particle interaction model

- ▶ Approximate a section of the DNA as a cylinder
- ▶ Use the energy dependent mean free path $\lambda(E)$ between successive ionisations to determine the distribution of clustered lesions [Van den Heuvel, 2014]
- ▶ Angular dependence: larger $\theta \implies$ longer path through DNA \implies higher LET and greater likelihood of inducing clustered damage

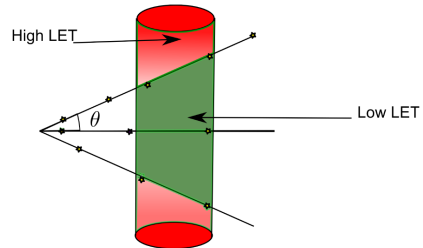


Figure: Image from Figure 1 in [Van den Heuvel, 2014].

Modeling DNA damage

Single particle interaction model

- ▶ Problem is equivalent to setting an isotropic point source at the boundary of the cylinder

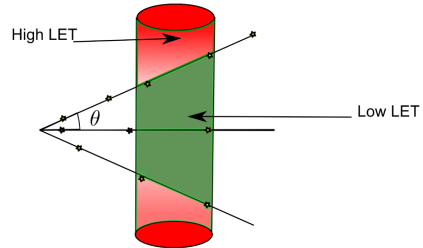


Figure: Image from Figure 1 in [Van den Heuvel, 2014].

Modeling DNA damage

Single particle interaction model

- ▶ Problem is equivalent to setting an isotropic point source at the boundary of the cylinder
- ▶ Reduces mathematically to that of the distribution of projections of a point source on a line-piece

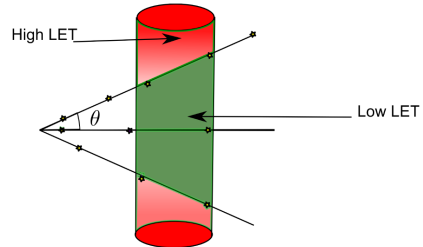


Figure: Image from Figure 1 in [Van den Heuvel, 2014].

Modeling DNA damage

Single particle interaction model

- ▶ Problem is equivalent to setting an isotropic point source at the boundary of the cylinder
- ▶ Reduces mathematically to that of the distribution of projections of a point source on a line-piece
- ▶ Solution: Cauchy distribution

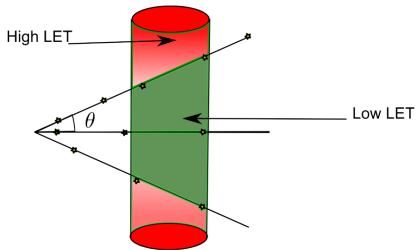


Figure: Image from Figure 1 in [Van den Heuvel, 2014].

Modeling DNA damage

Single particle interaction model

- ▶ Using $\lambda(E)$, the distribution of DSBs may be reformulated as a function of E instead of θ

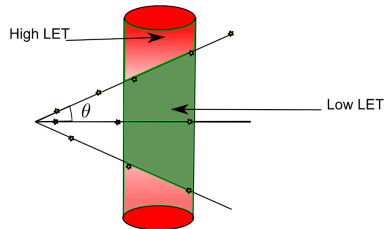


Figure: Image from Figure 1 in [Van den Heuvel, 2014].

Modeling DNA damage

Single particle interaction model

- ▶ Using $\lambda(E)$, the distribution of DSBs may be reformulated as a function of E instead of θ
- ▶ Damage response function: expected yield of DSBs given by [Van den Heuvel, 2014]

$$F_{cd}(E) = (a - b) \frac{2}{\pi} \left[\tan^{-1} \left(\frac{E - E_0}{\Gamma/2} \right) \right] + b \quad (3)$$

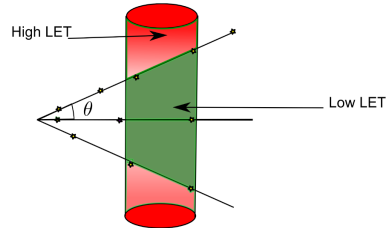


Figure: Image from Figure 1 in [Van den Heuvel, 2014].

Modeling DNA damage

Single particle interaction model

- ▶ Using $\lambda(E)$, the distribution of DSBs may be reformulated as a function of E instead of θ
- ▶ Damage response function: expected yield of DSBs given by [Van den Heuvel, 2014]

$$F_{cd}(E) = (a - b) \frac{2}{\pi} \left[\tan^{-1} \left(\frac{E - E_0}{\Gamma/2} \right) \right] + b \quad (3)$$

- ▶ Units: $\text{Gbp}^{-1}\text{Gy}^{-1}$

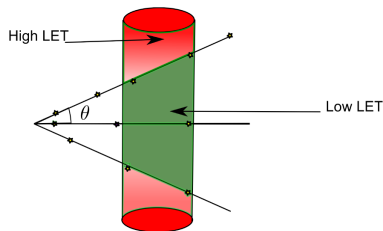


Figure: Image from Figure 1 in [Van den Heuvel, 2014].

Modeling DNA damage

Single particle interaction model

- ▶ Parameters a , b , Γ , and E_0 fitted through a two-stage χ^2 minimisation
- ▶ 1. Differential Lorentz distribution dF_{cd}/dE

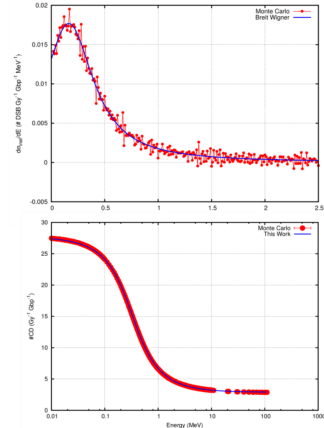


Figure: Images from Figures 3(b) and 4(b) in [Van den Heuvel, 2014].

Modeling DNA damage

Single particle interaction model

- ▶ Parameters a , b , Γ , and E_0 fitted through a two-stage χ^2 minimisation
- ▶ 1. Differential Lorentz distribution dF_{cd}/dE
- ▶ 2. Cumulative Cauchy distribution F_{cd}

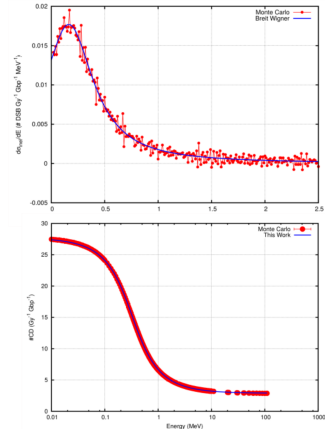


Figure: Images from Figures 3(b) and 4(b) in [Van den Heuvel, 2014].

Modeling DNA damage

Single particle interaction model

- ▶ Parameters a , b , Γ , and E_0 fitted through a two-stage χ^2 minimisation
- ▶ 1. Differential Lorentz distribution dF_{cd}/dE
- ▶ 2. Cumulative Cauchy distribution F_{cd}
- ▶ Good agreement with microscopic Monte Carlo software MCDS [Semenenko and Stewart, 2004]

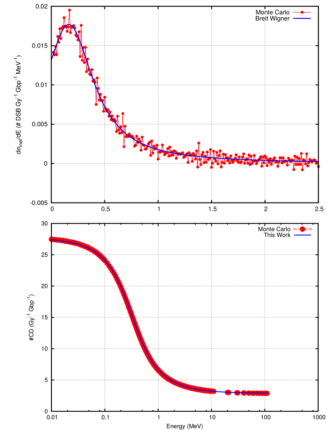


Figure: Images from Figures 3(b) and 4(b) in [Van den Heuvel, 2014].

Voxelised RBE distribution

- ▶ Dose deposited in each voxel $D[i,j,k]$ of the patient CT

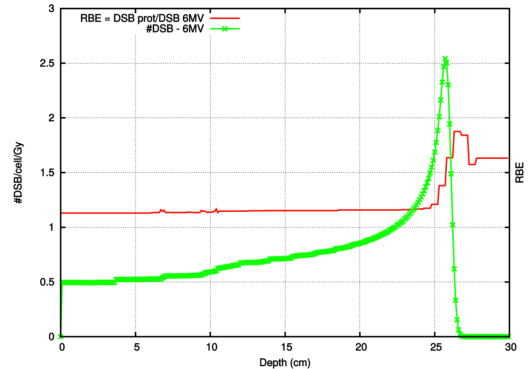


Figure: Image from Figure 6(b) in [Van den Heuvel, 2014].

Voxelised RBE distribution

- ▶ Dose deposited in each voxel $D[i,j,k]$ of the patient CT
- ▶ Energy spectrum $\Psi_{ijk}(E)$ in a voxel (by Monte Carlo or analytic models)

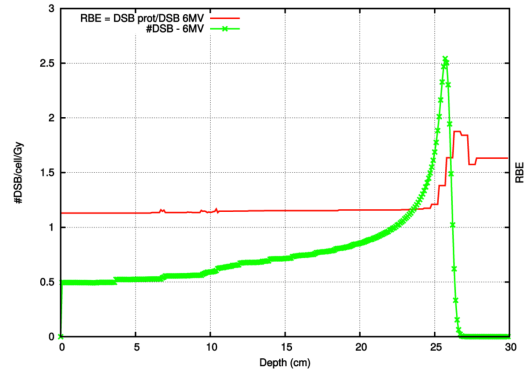


Figure: Image from Figure 6(b) in [Van den Heuvel, 2014].

Voxelised RBE distribution

- ▶ Dose deposited in each voxel $D[i, j, k]$ of the patient CT
- ▶ Energy spectrum $\Psi_{ijk}(E)$ in a voxel (by Monte Carlo or analytic models)
- ▶ Yield of complex damage $M_{cd}[i, j, k]$ can be calculated using the response function

$$M_{cd}[i, j, k] = D[i, j, k] \times \frac{\int_0^{E_{max}[i, j, k]} \Psi_{ijk}(E) F_{cd}(E) dE}{\int_0^{E_{max}[i, j, k]} \Psi_{ijk}(E) dE} \quad (4)$$

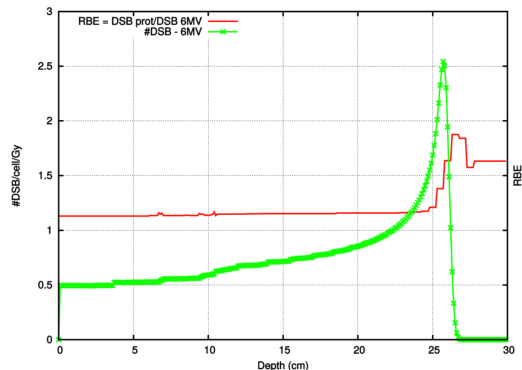


Figure: Image from Figure 6(b) in [Van den Heuvel, 2014].

Voxelised RBE distribution

- ▶ Dose deposited in each voxel $D[i, j, k]$ of the patient CT
- ▶ Energy spectrum $\Psi_{ijk}(E)$ in a voxel (by Monte Carlo or analytic models)
- ▶ Yield of complex damage $M_{cd}[i, j, k]$ can be calculated using the response function

$$M_{cd}[i, j, k] = D[i, j, k] \times \frac{\int_0^{E_{max}[i, j, k]} \Psi_{ijk}(E) F_{cd}(E) dE}{\int_0^{E_{max}[i, j, k]} \Psi_{ijk}(E) dE} \quad (4)$$

- ▶
$$RBE_{cd} = M_{cd,p} / M_{cd,\gamma} \quad (5)$$

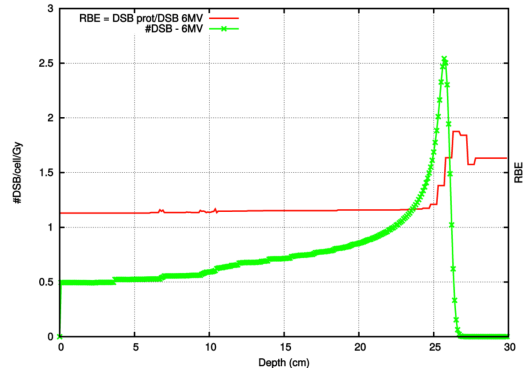
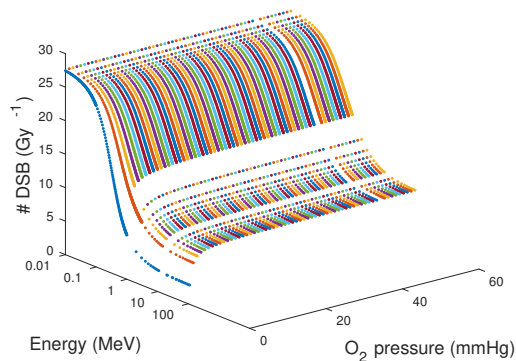


Figure: Image from Figure 6(b) in [Van den Heuvel, 2014].

Further considerations

Oxygen level modeling

- ▶ Amount of oxygen binding that can occur has a saturation behaviour

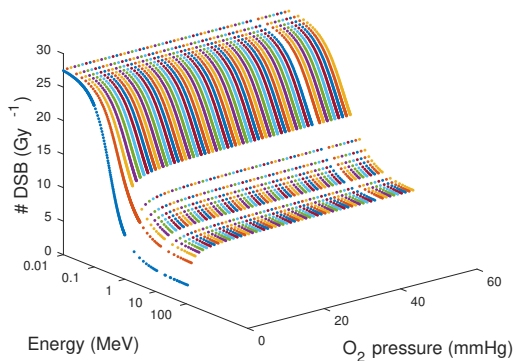


Further considerations

Oxygen level modeling

- ▶ Amount of oxygen binding that can occur has a saturation behaviour
- ▶ Can be modeled using second order D.E.
 [Kepner, 2010; Van den Heuvel, 2014]

$$\frac{(d^2y/dx^2)dx}{(dy/dx)} = N \left(\frac{dy}{y} \right) - M \left(\frac{dx}{x} \right) \quad (6)$$



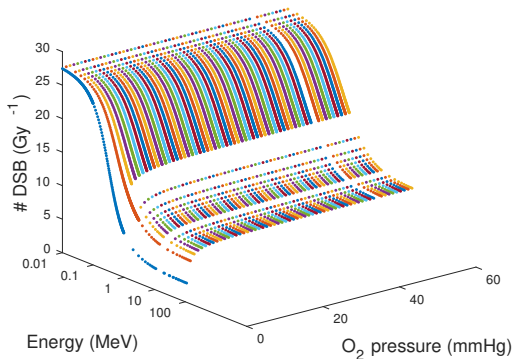
Further considerations

Oxygen level modeling

- ▶ Amount of oxygen binding that can occur has a saturation behaviour
- ▶ Can be modeled using second order D.E.
 [Kepner, 2010; Van den Heuvel, 2014]

$$\frac{(d^2y/dx^2)dx}{(dy/dx)} = N \left(\frac{dy}{y} \right) - M \left(\frac{dx}{x} \right) \quad (6)$$

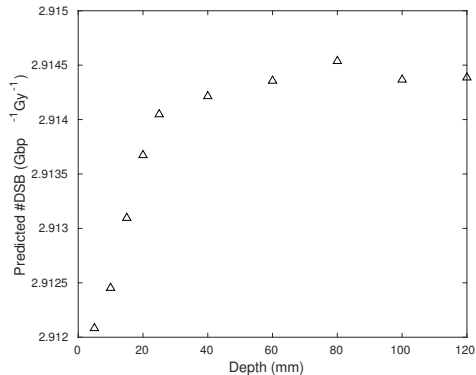
- ▶ In hypoxic conditions, only low-level damage component is reduced



Further considerations

Simplifying electron spectra

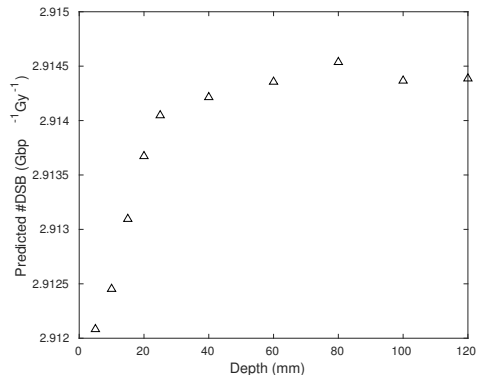
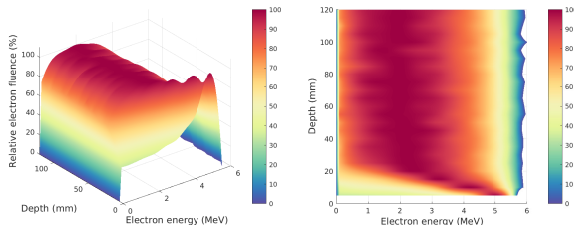
- ▶ Electronic build-up in entrance channel



Further considerations

Simplifying electron spectra

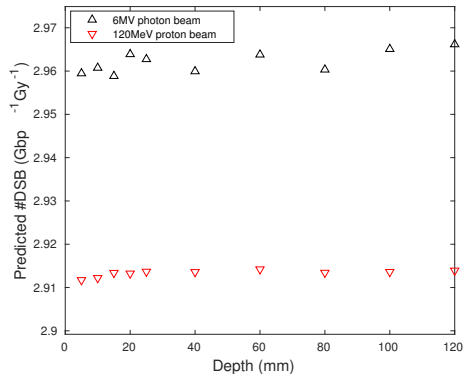
- ▶ Electronic build-up in entrance channel
- ▶ Otherwise, energy spectrum weakly dependent on depth



Further considerations

Simplifying electron spectra

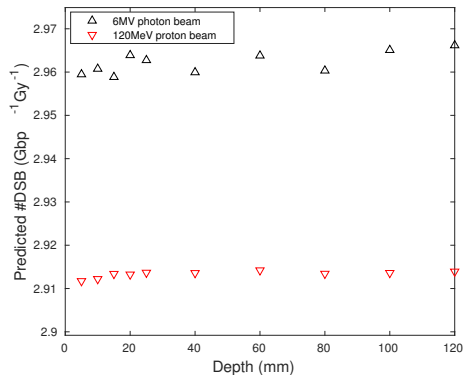
- ▶ Weak depth dependence seen in proton beam



Further considerations

Simplifying electron spectra

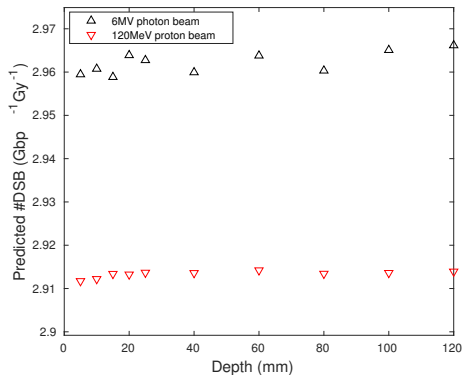
- ▶ Weak depth dependence seen in proton beam
- ▶ Resulting difference between electron-induced complex damage yield almost constant



Further considerations

Simplifying electron spectra

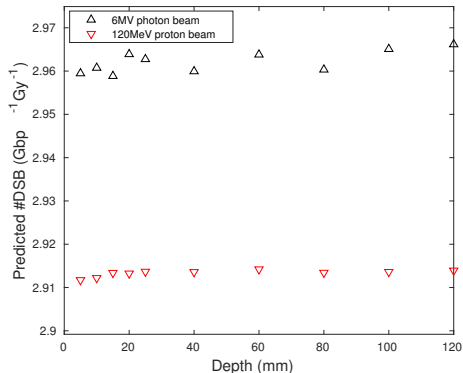
- ▶ Weak depth dependence seen in proton beam
- ▶ Resulting difference between electron-induced complex damage yield almost constant
- ▶ Consequence: only need to measure proton spectra



Further considerations

Simplifying electron spectra

- ▶ Weak depth dependence seen in proton beam
- ▶ Resulting difference between electron-induced complex damage yield almost constant
- ▶ Consequence: only need to measure proton spectra
- ▶ In Monte Carlo, can calculate $F_{cd}(E)$ on the fly for each history instead of obtaining a spectrum explicitly



Further considerations

Quantum chemistry and scattering

- ▶ Use density functional theory (DFT) to obtain electron distribution in small (10bp) segment of B-DNA

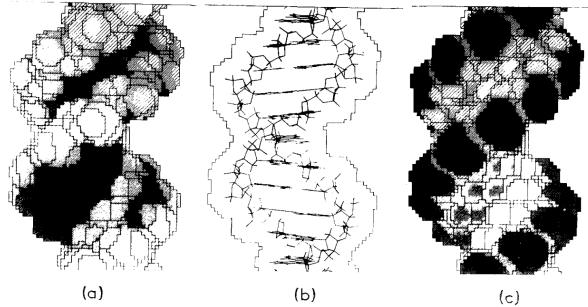


Fig. 2 : Potential (fig. 2a), a diagrammatic representation (fig. 2b) and the Field (fig. 2c) in a complete turn of a B-DNA double helix, with G-C base sequences. Significance of shadings :

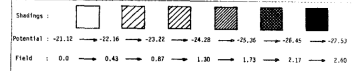


Figure: From [Pullman et al., 1983].

Further considerations

Quantum chemistry and scattering

- ▶ Use density functional theory (DFT) to obtain electron distribution in small (10bp) segment of B-DNA
- ▶ Calculate electrostatic potential map

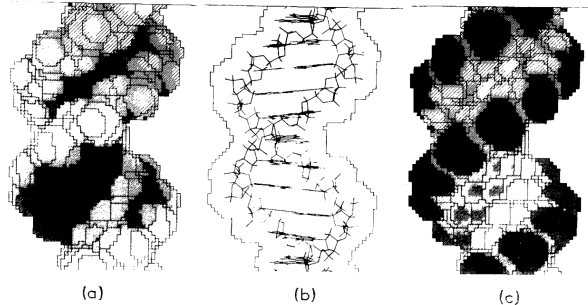


Fig. 2 : Potential (fig. 2a), a diagrammatic representation (fig. 2b) and the field (fig. 2c) in a complete turn of a B-DNA double helix, with G-C base sequences. Significance of shadings :

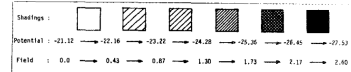


Figure: From [Pullman et al., 1983].

Further considerations

Quantum chemistry and scattering

- ▶ Use density functional theory (DFT) to obtain electron distribution in small (10bp) segment of B-DNA
- ▶ Calculate electrostatic potential map
- ▶ Find cross-section from scattering through Born series

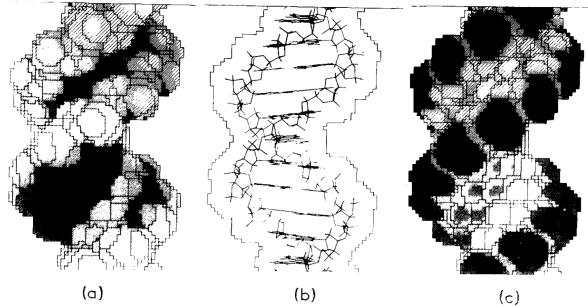


Fig. 2 : Potential (fig. 2a), a diagrammatic representation (fig. 2b) and the field (fig. 2c) in a complete turn of a B-DNA double helix, with G-C base sequences. Significance of shadings :

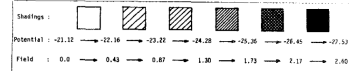


Figure: From [Pullman et al., 1983].

Further considerations

Quantum chemistry and scattering

- ▶ Use density functional theory (DFT) to obtain electron distribution in small (10bp) segment of B-DNA
- ▶ Calculate electrostatic potential map
- ▶ Find cross-section from scattering through Born series
- ▶ Second term in expansion is proportional to probability of two ionisation events within 10bp. This is labelled a DSB

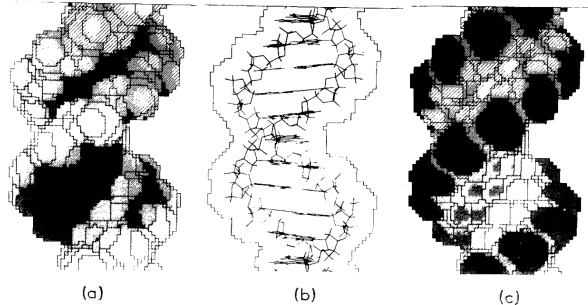


Fig. 2 : Potential (fig. 2a), a diagrammatic representation (fig. 2b) and the field (fig. 2c) in a complete turn of a B-DNA double helix, with G-C base sequences. Significance of shadings :

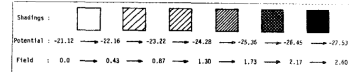


Figure: From [Pullman et al., 1983].

Further considerations

Quantum chemistry and scattering

- ▶ Use density functional theory (DFT) to obtain electron distribution in small (10bp) segment of B-DNA
- ▶ Calculate electrostatic potential map
- ▶ Find cross-section from scattering through Born series
- ▶ Second term in expansion is proportional to probability of two ionisation events within 10bp. This is labelled a DSB
- ▶ Use more terms for more clustered damage

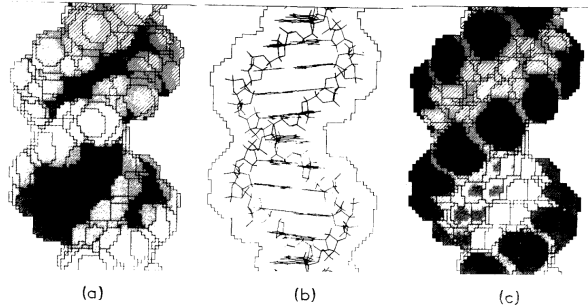


Fig. 2: Potential (fig. 2a), a diagrammatic representation (fig. 2b) and the field (fig. 2c) in a complete turn of a B-DNA double helix, with G-C base sequences. Significance of shadings:

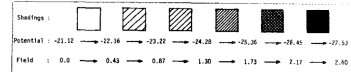


Figure: From [Pullman et al., 1983].

Summary of project aims

- ▶ Refine physical DNA-damage model

Summary of project aims

- ▶ Refine physical DNA-damage model
- ▶ Incorporate RBE into TPS on a voxel-by-voxel basis for proton and other particle (e.g. helium ion, carbon ion) therapies

Summary of project aims

- ▶ Refine physical DNA-damage model
- ▶ Incorporate RBE into TPS on a voxel-by-voxel basis for proton and other particle (e.g. helium ion, carbon ion) therapies
- ▶ Provide algorithmic framework for fast IMPT optimization (PTV- and robustness-based) which includes constraints on the RBE distribution.

Acknowledgements

This work was supported by Cancer Research UK grant number C2195/A25197, through a CRUK Oxford Centre DPhil Prize Studentship.

DPhil supervisors: Prof. Frank Van den Heuvel, Prof. Maria Hawkins, Dr. Francesca Fiorini

Radiation Therapy Medical Physics Group: Prof. Frank Van den Heuvel, Dr. Francesca Fiorini, Dr. Suliana Teoh, Dr. Ben George, Mark Brooke.

Many thanks to the General Sir John Monash Foundation, Cancer Research UK and the Clarendon Fund for supporting my studies.



References

- K. W. Caldecott. Single-strand break repair and genetic disease. *Nature Reviews Genetics*, 9:619–631, Aug 2008. URL <http://dx.doi.org/10.1038/nrg2380>. Review Article.
- M. Jermann. Particle therapy statistics in 2014. *International Journal of Particle Therapy*, 2(1):50–54, 2015. doi: 10.14338/IJPT-15-00013. URL <https://doi.org/10.14338/IJPT-15-00013>.
- G. R. Kepner. Saturation behavior: a general relationship described by a simple second-order differential equation. *Theoretical Biology and Medical Modelling*, 7(1):11, Apr 2010. ISSN 1742-4682. doi: 10.1186/1742-4682-7-11. URL <https://doi.org/10.1186/1742-4682-7-11>.
- M. Lomax, L. Folkes, and P. O'Neill. Biological consequences of radiation-induced dna damage: Relevance to radiotherapy. *Clinical Oncology*, 25(10):578 – 585, 2013. ISSN 0936-6555. doi: <https://doi.org/10.1016/j.clon.2013.06.007>. URL <http://www.sciencedirect.com/science/article/pii/S0936655513002471>. *Advances in Clinical Radiobiology*.
- A. Pullman, B. Pullman, and R. Lavery. Molecular electrostatic potential versus field. significance for dna and its constituents. *Journal of Molecular Structure: THEOCHEM*, 93:85 – 91, 1983. ISSN 0166-1280. doi: [https://doi.org/10.1016/0166-1280\(83\)80093-1](https://doi.org/10.1016/0166-1280(83)80093-1). URL <http://www.sciencedirect.com/science/article/pii/0166128083800931>. Proceedings of the XIIIth Congress of Theoretical Chemists of Latin Expression.
- V. A. Semenenko and R. D. Stewart. A fast monte carlo algorithm to simulate the spectrum of dna damages formed by ionizing radiation. *Radiation Research*, 161(4):451–457, 2004. ISSN 00337587, 19385404. URL <http://www.jstor.org/stable/3581187>.
- F. Van den Heuvel. A closed parameterization of dna-damage by charged particles, as a function of energy — a geometrical approach. *PLOS ONE*, 9(10):1–9, 10 2014. doi: 10.1371/journal.pone.0110333. URL <https://doi.org/10.1371/journal.pone.0110333>.
- J. F. Ward. Biochemistry of dna lesions. 104(2):S103–S111, 1985. doi: 10.2307/3576637. URL <http://ezproxy-prd.bodleian.ox.ac.uk:2084/stable/3576637>.